NIH Public Access
Author Manuscript
Dev Cell. Author manuscript; available in PMC 2010 June 1.

Published in final edited form as:
Dev Cell. 2009 June ; 16(6): 856–866. doi:10.1016/j.devcel.2009.04.005.

Metabolic control of oocyte apoptosis mediated by 14-3-3ζ-regulated dephosphorylation of caspase-2

Leta K. Nutt[1,*], **Marisa R. Buchakjian**[1,*], **Eugene Gan**[1], **Rashid Darbandi**[1], **Sook-Young Yoon**[3], **Judy Q. Wu**[1], **Yuko J. Miyamoto**[2], **Jennifer A. Gibbon**[1], **Josh L. Andersen**[1], **Christopher D. Freel**[1], **Wanli Tang**[1], **Changli He**[3], **Manabu Kurokawa**[1], **Yongjun Wang**[4], **Seth S. Margolis**[1], **Rafael A. Fissore**[3], and **Sally Kornbluth**[1]

1 *Department of Pharmacology and Cancer Biology, Duke University Medical Center, Durham, NC 27710*

2 *Department of Biology, Elon University, Elon, NC 27244*

3 *Department of Veterinary and Animal Sciences, University of Massachusetts, Amherst, MA 01003*

4 *Department of Medicine, Marion Bessin Liver Research Center, Albert Einstein College of Medicine, Bronx, NY 10461*

SUMMARY

Xenopus oocyte death is partly controlled by the apoptotic initiator, caspase-2. We reported previously that oocyte nutrient depletion activates caspase-2 upstream of mitochondrial cytochrome *c* release. Conversely, nutrient-replete oocytes inhibit caspase-2 via S135 phosphorylation catalyzed by calcium/calmodulin-dependent protein kinase II. We now show that caspase-2 phosphorylated at S135 binds 14-3-3ζ, thus preventing caspase-2 dephosphorylation. Moreover, we determined that S135 dephosphorylation is catalyzed by protein phosphatase-1, which directly binds caspase-2. Although caspase-2 dephosphorylation is responsive to metabolism, neither PP1 activity nor binding is metabolically regulated. Rather, release of 14-3-3ζ from caspase-2 is controlled by metabolism and allows for caspase-2 dephosphorylation. Accordingly, a caspase-2 mutant unable to bind 14-3-3ζ is highly susceptible to dephosphorylation. Although this mechanism was initially established in *Xenopus*, we now demonstrate similar control of murine caspase-2 by phosphorylation and 14-3-3 binding in mouse eggs. These findings provide an unexpected evolutionary link between 14-3-3 and metabolism in oocyte death.

Keywords

caspase-2; glucose-6-phosphate; protein phosphatase-1; 14-3-3; oocyte

INTRODUCTION

Apoptosis is a form of programmed cell death characterized by activation of cysteine proteases known as caspases, which dismantle the cell in an orderly, energy-dependent manner. Caspases are divided into two classes, initiator or effector, based on their position in the apoptotic

To whom correspondence should be addressed: E-mail: kornb001@mc.duke.edu, Phone: 919-613-8624, Fax: 919-681-1005.
*Contributed equally to this work

Publisher's Disclaimer: This is a PDF file of an unedited manuscript that has been accepted for publication. As a service to our customers we are providing this early version of the manuscript. The manuscript will undergo copyediting, typesetting, and review of the resulting proof before it is published in its final citable form. Please note that during the production process errors may be discovered which could affect the content, and all legal disclaimers that apply to the journal pertain.

NIH-PA Author Manuscript
NIH-PA Author Manuscript
NIH-PA Author Manuscript

NIH-PA Author Manuscript

NIH-PA Author Manuscript

NIH-PA Author Manuscript

hierarchy. Initiator caspases (e.g. caspases-2, -8, and -9) occupy the apical position in cell death pathways and are activated by dimerization, which involves recruitment of adaptor proteins to the caspase prodomain via homotypic interactions between their respective caspase recruitment domains (CARDs) (Danial and Korsmeyer, 2004). Once active, initiator caspases cleave and activate effector caspases to promote apoptosis.

In response to certain apoptotic cues, caspase-2 (C2) activation occurs on a platform consisting of the adaptor protein RAIDD, which binds directly to the C2 prodomain, and the death-domain-containing protein PIDD, which oligomerizes RAIDD (Baliga et al., 2004; Duan and Dixit, 1997; Read et al., 2002; Tinel and Tschopp, 2004). PIDD expression is p53-inducible and has been linked to genotoxic stress (Hanoux et al., 2007; Panaretakis et al., 2005; Robertson et al., 2002). Whether and how RAIDD or PIDD might be regulated post-translationally to control apoptosis is unknown.

The nutrient status of a cell may be important in the decision to initiate apoptosis. Decreased glucose uptake and glycolytic rate occur upon growth factor withdrawal in lymphocytes, and this precedes commitment to caspase activation (Rathmell et al., 2003). Artificial maintenance of glycolysis confers apoptotic resistance under these conditions (Zhao et al., 2007). Furthermore, AKT kinase exerts an anti-apoptotic effect in many cell types and requires glucose uptake in order to do so (Majewski et al., 2004; Pastorino et al., 2002; Rathmell et al., 2003; Zhao et al., 2007). When hexokinase is bound to mitochondria it can suppress the pro-apoptotic release of mitochondrial cytochrome *c* (cyt *c*) (Majewski et al., 2004; Pastorino et al., 2002). It has also been demonstrated that the pro-apoptotic Bcl-2 family member, BAD, forms a complex with and regulates the activity of glucokinase at the mitochondria (Danial et al., 2003).

We reported previously that nutrient depletion in *Xenopus* oocytes promotes apoptosis through activation of C2 (Nutt et al., 2005). This is particularly interesting in light of work by Yuan et al. demonstrating that the primary phenotype of C2 knockout mice is excess oocytes in females, suggesting that oocytes might be particularly susceptible to C2-mediated death (Bergeron et al., 1998). In exploring links between metabolism and C2, we discovered that maintenance of NADPH levels by flux through the pentose phosphate pathway (PPP) induces a suppressive phosphorylation of *Xenopus* C2 on S135. A non-phosphorylatable mutant of C2 (S135A) induced apoptosis even in the presence of high levels of NADPH.

In analyzing regulation of C2, we found that NADPH promotes activation of calcium/calmodulin-dependent protein kinase II (CaMKII), which catalyzes S135 phosphorylation. Thus, for oocytes to undergo apoptosis upon nutrient depletion (decreasing PPP flux), a phosphatase must be required to dephosphorylate C2. Although a large number of kinases have been implicated in apoptotic regulation, potential links between phosphatases and cell death are poorly understood. For protein phosphatases-1 and -2A, specificity is typically conferred by a targeting subunit which either directs the catalytic subunit to its substrates or alters its subcellular localization (Cohen, 2002; Shenolikar, 1994). Recently, however, it has been shown that the PP1 catalytic subunit may also bind directly to substrates via substrate motifs similar to those found on targeting subunits (Margolis et al., 2003; Vietri et al., 2006). In these cases, targeting subunits may be dispensable for dephosphorylation. Regulation of PP1 activity and specificity may furthermore occur through PP1 binding to inhibitory proteins (I1, I2), and substrate dephosphorylation may also be modulated by additional post-translational modifications and/or binding partners. We recently reported this mechanism for the cell cycle phosphatase Cdc25 (Margolis et al., 2006). In this example, 14-3-3 protein binds to Cdc25, masking PP1 access to phospho-S287. Cdc25 remains phosphorylated and suppressed until 14-3-3 dissociates, thus leaving S287 vulnerable to PP1 (Margolis et al., 2006; Margolis et al., 2003).

NIH-PA Author Manuscript

NIH-PA Author Manuscript

NIH-PA Author Manuscript

Although NADPH is required for apoptotic suppression in the oocyte, it is not known if C2 activation might also be a locus of metabolic control. We now demonstrate that PP1-mediated C2 dephosphorylation is required for C2 activation, and dephosphorylation is indirectly regulated by PPP flux. In searching for novel C2 prodomain interactors, we discovered that 14-3-3ζ binds the C2 prodomain. Moreover, S135 dephosphorylation, which is required for C2 activation, depends upon removal of 14-3-3ζ. Importantly, 14-3-3ζ removal is under tight metabolic control; stimulation of the PPP results in 14-3-3ζ binding, and nutrient depletion promotes 14-3-3ζ release. Finally, we have also uncovered evidence of a parallel regulatory C2 activation pathway in mammalian oocytes, in that perturbation of murine C2 phosphorylation or 14-3-3 binding appears to control the viability of mouse eggs. These data provide evidence that the metabolic regulation of C2 activation depends upon an evolutionarily conserved association with 14-3-3, and this association mediates the phosphorylation status and activity of C2 during apoptosis in the oocyte.

RESULTS

Metabolic suppression of caspase-2 dephosphorylation

Our previous work indicated that nutrient abundance inhibited C2 through CaMKII-mediated S135 phosphorylation. These findings, coupled with observations placing C2 upstream of mitochondrial cyt *c* release, implied that C2 should be dephosphorylated prior to caspase-3 (C3) activation. To evaluate this we monitored the phosphorylation status of endogenous C2 in egg extracts using an antibody directed against phosphorylated S135 (Fig. 1A). Endogenous C2 was immunoprecipitated using either a *Xenopus* C2 antibody directed against the C-terminal 20 amino acids of the protein or the corresponding preimmune serum, and immunoprecipitates were analyzed for C2 pS135. This experiment was performed in the presence of the C2 inhibitor VDVAD-CHO to ensure that loss of C2 pS135 was not due to C2 processing. As shown in Figure 1B, endogenous C2 was dephosphorylated at S135 over time, and this preceded C3 activation.

These observations raised the interesting possibility that an S135-directed phosphatase might be regulated by metabolism, thus activating C2 upon nutrient depletion. To examine C2 dephosphorylation in isolation we prepared radiolabeled, S135-phosphorylated C2 prodomain (pro) fused to GST as a dephosphorylation substrate. Incubation of this construct in egg extract resulted in dephosphorylation of C2 S135 immediately preceding C3 activation, as would be expected if C2 dephosphorylation was required for its own activation and downstream caspase activity (Fig. 1C; the time course of C3 activation differs between extracts, but C2 dephosphorylation prior to C3 activation was consistent across multiple extracts). When we repeated this assay in the presence of G6P to increase PPP activity, C2 dephosphorylation and C3 activation were inhibited (Fig. 1D and Supplemental Data, Fig. 1). These data suggested that C2 dephosphorylation and activation were under metabolic control.

We also show that dephosphorylation of GST-C2 pro preceded C2 activation as demonstrated by processing of *in vitro* translated full-length C2 (Fig. 1E). These data suggested that both endogenous full-length and isolated pro-C2 were dephosphorylated at S135 over time, and this preceded C2 processing and C3 activation.

PP1 interacts with caspase-2 prodomain

To identify the phosphatase responsible for C2 dephosphorylation, we titrated the phosphatase inhibitor okadaic acid (OA) into extracts and monitored C3 activation, mitochondrial cyt *c* release, GST-C2 pro dephosphorylation, and full-length C2 processing (Figs. 2A–C). OA follows a biphasic dose response curve in the extract, with nM/low μM doses inhibiting PP2A and higher (~10 μM) concentrations inhibiting PP1 (Margolis et al., 2003). OA doses known

NIH-PA Author Manuscript

NIH-PA Author Manuscript

NIH-PA Author Manuscript

to inhibit PP1 but not those inhibiting only PP2A abrogated C3 activation, cyt *c* release, and C2 dephosphorylation (Figs. 2A and B). 10 μM OA also prevented processing of full-length C2 (Fig. 2C). These data (and the fact that >95% of OA-inhibitable phosphatases in the extract is PP1 or PP2A) strongly suggested that PP1 might dephosphorylate C2 S135.

To confirm that PP1 was the S135-directed phosphatase we depleted extract of endogenous PP1 using GST-I2 as an affinity resin and monitored samples for GST-C2 pro dephosphorylation. As shown in Figure 2D, PP1 depletion markedly inhibited C2 dephosphorylation. Also consistent with a role for PP1, GST-C2 pro was able to bind PP1 in extracts but not PP2A (Fig. 2E), and we also did not observe binding to the OA-inhibitable phosphatase PP5 (data not shown). Additionally, endogenous C2 co-immunoprecipitated with endogenous PP1 (Fig. 2G).

PP1 is commonly directed to its substrates by a targeting subunit (Cohen, 2002). We reasoned that a targeting subunit involved in C2 dephosphorylation would be a component of the PP1-C2 complex. Thus, GST-C2 pro was incubated in extract and bound proteins were analyzed via far western assay with digoxigenin-labeled PP1. Interestingly, we did not see binding of PP1 to any protein in the affinity precipitate other than C2 pro itself (data not shown). These data were reminiscent of previous work from our lab demonstrating that PP1 directly binds Cdc25 in the absence of a targeting subunit (Margolis et al., 2003). Similar results have also been reported for the retinoblastoma protein (Vietri et al., 2006). Therefore, we hypothesized that PP1 might mediate S135 dephosphorylation through direct C2 binding. To test this we examined the interaction between GST-C2 pro and recombinant PP1 catalytic domain. As shown in Figure 2F (right two lanes), GST-C2 pro bound directly to recombinant PP1 *in vitro*, consistent with the idea that PP1 and C2 interact in the absence of a targeting subunit.

PP1 binding is required for caspase-2 activation

Only a handful of PP1 substrates have been shown to bind PP1 directly (Margolis et al., 2003; Vietri et al., 2006). Analyses of PP1 binding motifs on direct substrates and targeting subunits have identified VxF as a PP1 docking site (Egloff et al., 1997; Wakula et al., 2003). We scanned C2 pro for VxF motifs and failed to identify a candidate, however, we mutated several valines and downstream residues in the hope that these residues might cooperate to confer PP1 docking. As shown in Figures 3A and B, mutation of V18/L20 and V106/H108 demonstrated that V106A/H108A disrupted PP1 binding both in extract and in buffer. This double mutant was phosphorylated by CaMKII to the same extent as WT (Fig 3C). To determine if PP1 binding was essential for C2 dephosphorylation, we assayed dephosphorylation of these mutants over time. We found that V106A/H108A was markedly refractory to dephosphorylation, while V18A/L20A was rapidly dephosphorylated (Fig. 3D). Moreover, V18A/L20A demonstrated metabolic regulation similar to WT C2 pro (Figure 3D). Consistent with these observations, microinjection of flag-tagged, full-length C2 V106A/H108A mRNA into *Xenopus* oocytes did not effectively induce death, whereas an equivalent amount of WT protein readily killed the oocytes (Figs. 3E and F).

Although C2 dephosphorylation was under metabolic control and mediated by PP1, this did not necessarily indicate that this interaction was controlled by metabolism. Therefore, we wished to determine whether PP1 bound C2 constitutively or whether binding was induced just prior to caspase activation. As shown in Figure 3G, GST-C2 pro bound PP1 constitutively, and binding was not reduced by G6P (also see Fig. 2F, first 4 lanes). More importantly, when His-tagged PP1 was incubated in control- or G6P-treated extracts, retrieved, and then incubated with CaMKII-phosphorylated GST-C2 pro *in vitro*, we saw that C2 was dephosphorylated to a similar degree regardless of G6P treatment (Fig. 3H, first four lanes). Thus, although C2 dephosphorylation was metabolically regulated, regulation was not at the level of phosphatase activity or binding.

NIH-PA Author Manuscript

NIH-PA Author Manuscript

NIH-PA Author Manuscript

14-3-3ζ binds caspase-2

Since C2 dephosphorylation was regulated by metabolism but the C2/PP1 interaction and PP1 activity were not, we hypothesized that an additional factor(s) must be involved. To identify C2 interactors we used C2 pro as bait in a yeast two-hybrid screen and identified the phosphoserine binding protein 14-3-3ζ. In agreement with this finding, we determined that GST-C2 pro bound endogenous 14-3-3 in G6P-treated extract (Fig. 4A). In a converse experiment, it was determined that binding of endogenous C2 to GST-14-3-3ζ but not ε was enhanced in the presence of G6P (Fig. 4B), however, there did appear to be some constitutive background binding to 14-3-3ε. Given this observation, we confirmed that 14-3-3ζ preferentially bound CaMKII-phosphorylated C2 by phosphorylating GST-C2 pro at S135 *in vitro* and incubating it with different 14-3-3 isoforms. We show in Figure 4C that GST-C2 pro pS135 bound 14-3-3ζ but not a 14-3-3ζ mutant unable to bind target proteins (14-3-3ζ K49E) or 14-3-3ε (Zhang et al., 1997). These results suggested that C2 selectively binds 14-3-3ζ when nutrients are abundant.

These observations raised the possibility that binding of 14-3-3ζ might control C2 activation. In this regard, it was interesting that release of pre-bound endogenous 14-3-3ζ from GST-C2 pro in extract was observed to occur before C3 activation (Fig. 4D). Furthermore, addition of excess His-14-3-3ζ blocked full-length C2 processing, whereas equal amounts of 14-3-3ζ K49E or 14-3-3ε were unable to do so (Fig. 4E). Finally, addition of excess 14-3-3ζ to extract also prevented C3 activation (Fig. 4F). These data suggested that 14-3-3ζ binding might, indeed, control C2 activation.

14-3-3ζ binding regulates caspase-2 dephosphorylation

As described above, our lab reported that cell cycle-regulated activation of Cdc25 depends upon 14-3-3 release (Margolis et al., 2006; Margolis et al., 2003). We speculated that C2 dephosphorylation might also be regulated at the level of 14-3-3 release, particularly because PP1 did not appear to be under metabolic control. To address this we first examined the timing of 14-3-3 release from GST-C2 pro compared to dephosphorylation. As shown in Figure 5A, 14-3-3ζ released from C2 pro prior to maximal C2 dephosphorylation. Next, we examined GST-C2 pro dephosphorylation in the presence of excess His-14-3-3ζ WT or K49E. We saw that prephosphorylated GST-C2 pro was dephosphorylated in control extract or extract with 14-3-3ζ K49E, but dephosphorylation was significantly decreased in the presence of excess 14-3-3ζ WT (Fig. 5B). This experiment suggested that the inhibitory effect of 14-3-3ζ on C2 is directly related to the interaction between the two.

Mutation of GST-C2 pro S135 to Ala abrogated 14-3-3ζ binding through loss of the phosphoserine docking site, and binding was also lost when C2 pro D137 was mutated to Ala, thus disrupting the downstream sequence required for efficient interaction (Fig. 5C). It is important to note that the C2/14-3-3ζ binding motif is non-canonical in nature: classical 14-3-3 binding sequences are defined as RSXpSXP (mode I) and RXY/FXpSXP (mode II), although the literature suggests considerable binding site degeneracy (Rittinger et al., 1999;Yaffe et al., 1997;Yang et al., 2006). Although canonical motifs are thought to confer high-affinity binding, 14-3-3 interactions with atypical motifs may result in binding subject to novel regulation, which appears to be the case for metabolic regulation of C2 (Yaffe et al., 1997).

If 14-3-3ζ binding controlled C2 dephosphorylation, we would expect C2 D137A to be dephosphorylated more rapidly than WT. We first confirmed that CaMKII was able to phosphorylate GST-C2 pro WT and D137A to the same extent *in vitro* (Fig. 5D). Next, GST-C2 pro WT or D137A was prephosphorylated with CaMKII and incubated in extract, and GST-C2 pro phosphorylation status was assessed. As shown in Figure 5E, C2 D137A was dephosphorylated more rapidly than WT, consistent with a role for 14-3-3ζ in inhibition of C2

NIH-PA Author Manuscript

NIH-PA Author Manuscript

NIH-PA Author Manuscript

dephosphorylation. We also depleted extract of PP1 using GST-I2, demonstrating that PP1 is required for C2 D137A dephosphorylation (Fig. 5F). We were able to reinforce these conclusions *in vitro* using recombinant components; addition of excess His-14-3-3ζ was sufficient to block dephosphorylation of GST-C2 pro by His-PP1 in buffer (Fig. 3H, last two lanes). In agreement with the idea that 14-3-3ζ binding controls C2 dephosphorylation (rather than vice versa), addition of sufficient OA to inhibit PP1 did not interfere with 14-3-3ζ release, suggesting that these are separable events (Fig. 5G, upper panel).

14-3-3ζ release is metabolically regulated

As described above, G6P blocks C2 dephosphorylation and activation, yet PP1 was not metabolically regulated. Since S135 dephosphorylation was more rapid in the absence of 14-3-3ζ, this suggested that metabolic suppression of C2 might result from a block in 14-3-3ζ removal. As shown in Figure 5H, 14-3-3ζ release from GST-C2 pro was suppressed in the presence of G6P even with CaMKII inhibition, demonstrating that CaMKII activity and 14-3-3ζ release are completely separable. Finally, if 14-3-3ζ removal is the point of metabolic control, then C2 D137A should not be susceptible to metabolic suppression of C2 pS135. This was, in fact, the case as dephosphorylation of GST-C2 pro D137A rapidly proceeded regardless of G6P treatment. Moreover, D137 dephosphorylation occurred despite inhibition of cyt *c* release by Bcl-xL to prevent downstream apoptotic events (Fig. 6A; note that G6P and Bcl-xL were used at sufficient concentrations to suppress endogenous apoptosis). We also show in Figure 6B that *in vitro* translated full-length C2 D137A was readily processed in the presence of G6P whereas C2 WT was not, demonstrating that 14-3-3ζ binding was critical for C2 suppression by metabolism.

Furthermore, GST-C2 pro D137A prephosphorylated at S135 was readily susceptible to recombinant PP1 *in vitro*, demonstrating that this mutation did not interfere with PP1 binding or activity (Fig. 6C). Consistent with these observations, microinjection of full-length C2 D137A mRNA into *Xenopus* oocytes induced death more robustly than injection of WT (Fig. 6D). Therefore, activation of C2 upon nutrient depletion relies upon removal of 14-3-3ζ; when this point of control cannot be exerted (D137A mutant), C2 activation is uncoupled from the nutrient status of the cell.

Metabolic regulation of caspase-2 is conserved in the mammalian oocyte

Although our data indicated that C2 phosphorylation and 14-3-3 binding were crucial for inhibition of *Xenopus* oocyte death, we wished to determine whether this might also be important for mouse oocyte survival, particularly given the presence of excess oocytes in C2 knockout mice (Bergeron et al., 1998). We first identified a metabolically-regulated phosphorylation site on mouse C2 (mC2). Since it is impossible to obtain sufficient mouse oocytes for biochemical experiments, we used *Xenopus* egg extract as a tool for identifying mC2 phosphorylation sites. Incubation of GST-mC2 pro WT or candidate phospho-mutants in extract with G6P identified S164 as a potential site (Fig. 7A). Moreover, an *in vitro* CaMKII assay also suggested that GST-mC2 pro S164 might be a CaMKII target (Fig. 7B). Furthermore, GST-mC2 pro S164A was shown to be deficient in 14-3-3 binding, and a 14-3-3 binding mutant analogous to *Xenopus* C2 D137A (D166A) was validated (Fig. 7C; it is important to note that like *Xenopus* C2, the mC2 14-3-3-binding sequence is also non-canonical). We tested full-length mC2 constructs by microinjection into *Xenopus* oocytes and observed that mC2 S164A behaved much like *Xenopus* C2 S135A in inducing robust oocyte death (Figs. 7D and E).

In *Xenopus* oocytes, NADPH generation by the PPP promotes CaMKII activity and phosphorylation of C2 S135. Accordingly, we previously reported that full-length C2 WT mRNA injected into oocytes was rapidly suppressed via PPP flux (Nutt et al., 2005). In contrast, concomitant microinjection of a CaMKII inhibitor, negating the contribution of NADPH,

NIH-PA Author Manuscript

NIH-PA Author Manuscript

NIH-PA Author Manuscript

enhanced the potency of C2. To determine if similar regulation was conserved in mammals, we examined mC2 in the context of mouse egg apoptosis. In fresh postovulatory mouse eggs where we would expect abundant NADPH and CaMKII activity, overexpression of full-length mC2 WT induced death more slowly than mC2 S164A (homologous to *Xenopus* S135, Fig. 7F). Also similar to *Xenopus* C2, the mC2 14-3-3 binding mutant was more potent than WT (Fig. 7G).

A decrease in G6P dehydrogenase activity has been demonstrated in aged mouse oocytes (de Schepper et al., 1987). Therefore, we speculated that age-related decreases in PPP flux might sensitize mouse eggs to C2-dependent death. As predicted, postovulatory aged eggs were markedly more susceptible than fresh eggs to death induced by WT C2 (Figs.7H and I; note that mC2 S164A and D166A were also more potent in aged oocytes as expected, suggesting that additional cell death-inhibitory factors may be inactivated, or stimulatory factors activated during aging). These data demonstrated that our observations in *Xenopus* oocytes were conserved in the murine egg, suggesting that decreases in metabolism may contribute to oocyte death during aging.

DISCUSSION

The role of C2 in oocyte death was established by experiments demonstrating that C2 knockout mice are characterized by excess oocytes (Bergeron et al., 1998). Subsequently, we have reported that C2 is inhibited when oocyte nutrients are sufficient to stimulate PPP-mediated NADPH production, which promotes CaMKII-mediated phosphorylation and inhibition of C2. In this report, we demonstrate that C2 activation is also under tight metabolic control. Removal of the suppressive C2 S135 phosphorylation is catalyzed by PP1, but this step is not metabolically regulated. Rather, the point of metabolic control is at the level of 14-3-3ζ, whose removal from C2 is required for S135 dephosphorylation. These observations suggest that C2 is dormant in nutrient-replete oocytes until stockpiles are exhausted, thus engaging a 14-3-3-release pathway to activate C2 and trigger oocyte death.

We have now demonstrated that PP1 is the C2 S135-directed phosphatase. The interaction between C2 and PP1 is both direct and constitutive, and we have mapped the PP1 binding site as C2 V106/H108. Mutation of this site prevents PP1 binding and C2 dephosphorylation. Thus, C2 joins a small list of proteins regulated by PP1 in the absence of a targeting subunit.

Since PP1 binding and activity toward C2 are independent of metabolism, we deduced that an additional factor(s) must dictate C2 phosphorylation under these conditions. We now show that 14-3-3ζ binding to C2 is under metabolic control, and a C2 mutant unable to bind 14-3-3ζ is dephosphorylated regardless of nutrient status. Therefore, factors controlling 14-3-3ζ removal from C2 are critical for metabolic control of oocyte apoptosis.

The mechanism underlying 14-3-3ζ release from C2 is not yet clear. 14-3-3 binding regulates the activity of many pro-apoptotic proteins, and in these cases its release depends upon post-translational modification (e.g. JNK phosphorylates 14-3-3 promoting its release from BAD and BAX) (Datta et al., 2000; Nomura et al., 2003; Sunayama et al., 2005; Tsuruta et al., 2004; Zha et al., 1996). We have not observed phosphorylation of 14-3-3ζ in extract prior to its release from C2. GST-C2 pro phosphorylated at S135 and incubated in nutrient-deplete extract (treated with DHEA to inhibit PPP) is deficient in *in vitro* binding of recombinant 14-3-3ζ, but similarly incubated GST-14-3-3ζ protein retains its ability to bind *in vitro* translated, phosphorylated C2 (LKN and SK, unpublished). It may be that any post-translational modification necessary for 14-3-3ζ release is targeted to C2 itself. We also do not observe C2 pro phosphorylation outside of S135, suggesting that distinct post-translational C2 modifications or prodomain binding factors may play a role in 14-3-3ζ release.

NIH-PA Author Manuscript

NIH-PA Author Manuscript

NIH-PA Author Manuscript

In the *Xenopus* oocyte, overexpression of full-length C2 S135A was a potent inducer of apoptosis when compared to WT. Young, healthy oocytes contain substantial internal nutrients, and as such we hypothesized that C2 was suppressed by S135 phosphorylation as it was translated (Nutt et al., 2005). Extending these studies to the mouse egg, we have now identified a homologous site on mC2 that appears to be important in the metabolic regulation of mouse egg apoptosis. It is currently not clear if somatic mC2 is also regulated through S164 phosphorylation or if this pathway is exclusive to oocytes.

In fresh mouse eggs expected to have robust PPP and CaMKII activity, overexpression of full-length mC2 WT induced death more weakly than either the phospho- or 14-3-3-binding mutants. It has been suggested that activity of the rate-limiting step in the PPP (G6P dehydrogenase) markedly decreases with age in mouse oocytes (de Schepper et al., 1987). Along those lines, we demonstrated that postovulatory aged mouse eggs were substantially more sensitive to injection of mC2 than fresh eggs, most likely due to a decrease in NADPH-dependent CaMKII activity. Given these data, it is attractive to speculate that a loss of PPP operation *in vivo* may underlie oocyte depletion in females as they age: over time, oocytes lose G6P dehydrogenase activity, thus promoting a drop in NADPH and concomitant loss of CaMKII activity. This would, in essence, remove the metabolic impediment to 14-3-3 release, thus priming C2 for PP1-mediated dephosphorylation and activation and leaving the oocyte readily susceptible to apoptosis induced by a variety of stressors (e.g. oxidative damage, waning hormonal stimulation). Taken together, our observations also raise the interesting possibility that pathologic alterations in C2-directed PP1 activity or changes in 14-3-3ζ levels could contribute to changes in female fertility.

EXPERIMENTAL PROCEDURES

Xenopus extract and oocytes

Mature female frogs were induced to lay eggs as described previously (Smythe and Newport, 1991). Jelly coats were removed with 2% cysteine (pH 8.0) and eggs were washed ×3 with modified Ringer's solution (MMR: 1 M NaCl, 20 mM KCl, 10 mM $MgSO_4$, 25 mM $CaCl_2$, 5 mM Hepes, pH 7.8, 0.8 mM EDTA) and ×3 in egg lysis buffer (ELB: 250 mM sucrose, 2.5 mM $MgCl_2$, 1.0 mM dithiothreitol, 50 mM KCl, 10 mM Hepes, pH 7.7). Eggs were centrifuged at 400 *g*, and cytochalasin B (5 μg/mL; Calbiochem), aprotinin/leupeptin (5 μg/mL), and cyclohexamide (50 μg/mL) were added. Lysis was performed by centrifugation at 10,000 *g*, 12 min. Crude cytosolic egg extracts were supplemented with 2 mM ATP and 20 mM phosphocreatine.

Stage VI oocytes were prepared from frogs primed with pregnant mare serum gonadotropin 3–5 days before excision of ovaries. Ovaries were digested with 2.8 U liberase (Roche) in OR-2 buffer (82.5 mM NaCl, 2 mM KCl, 1 mM $MgCl_2$, 5 mM HEPES, pH 7.5) for 1.5 hr at room temperature (RT). Oocytes were washed with OR-2 buffer and stored in OR-2 + 1% fetal bovine serum, 0.2% gentamicin overnight at 18°C. Healthy stage VI oocytes were selected for microinjection.

Recombinant protein cloning and expression

pGEXKG N-terminal GST-*Xenopus* C2 pro, mC2 pro, 14-3-3ζ and ε, I2, and His-PP1 were expressed in BL21 *E. coli* as described previously (Gasco et al., 2002).

Xenopus C2 was cloned as previously described into pGEXKG and pSP64T (Nutt et al., 2005). The Quikchange kit (Stratagene) was used to generate *Xenopus* C2 mutants from the WT template using the primers detailed in Supplemental Data.

NIH-PA Author Manuscript

NIH-PA Author Manuscript

NIH-PA Author Manuscript

To produce radiolabeled *in vitro* translated protein, pSP64T C2 cDNA was added at 20 ng/μL to rabbit TNT reticulocyte lysate (Promega) containing 0.4 μCi/μL ^{35}S-Translabel, 1× (minus-Cys, minus-Met) amino acid mix, and additional components in accordance with the manufacturer's protocol.

Antibodies

Anti-PP1 (polyclonal, 1:1000) and PP2A (monoclonal, 1:2000) were purchased from Upstate; anti-cyt *c* (polyclonal, 1:500) from Pharmingen; anti-14-3-3 (polyclonal, 1:1000) from AbCam, anti-actin (monoclonal, 1:4000) from Sigma-Aldrich, anti-flag (polyclonal, 1:1000) from Cell Signaling, anti-CaMKII pT286 (polyclonal, 1:1000) from AbCam, and anti-CaMKII (monoclonal, 1:1000) from BD Transduction Laboratories. *Xenopus* polyclonal antibodies were generated as described in Supplemental Data.

Caspase Assay

3 μL egg extract was incubated in 90 μL DEVDase buffer (50 mM Hepes, pH 7.5, 100 mM NaCl, 0.1% CHAPS, 10 mM DTT, 1 mM EDTA, 10% glycerol) with the colorimetric peptide substrate Ac-DEVD-pNA (200 mM final concentration; BIOMOL Research Labs, Inc.). Reactions were incubated at 37 °C for 30 min. Absorbance of the colorimetric product was measured at 405 nm using a BioRad microplate reader.

Caspase-2 dephosphorylation assay

30 μg GST-C2 pro was phosphorylated at S135 as follows: glutathione sepharose-bound proteins were incubated with recombinant CaM and CaMKII in CaMK buffer (1 M Hepes, pH 7.5, 1 M DTT, 1 M $MgCl_2$, 10% Tween, 0.2 M ATP, 1 M $CaCl_2$) in the presence of 10 μCi [γ-^{32}P]ATP. Radiolabeled GST-C2 pro was then incubated in extract at RT. Samples were washed with buffer containing salt and detergent, eluted with SDS sample buffer, resolved on SDS-PAGE, and analyzed by autoradiography.

Cytochrome *c* release assay

15 μL crude extract was diluted in 15 μL ELB and filtered through a 0.1 μm ultrafree-MC filter (Millipore). The filtrate was mixed with SDS sample buffer, resolved by 17.5% SDS-PAGE, and transferred to PVDF membrane (Millipore, Bedford, MA). The membrane was probed with an anti-cyt *c* antibody.

Inhibitor-2 affinity depletion of PP1

Xenopus extract was depleted of PP1 by three one-hour incubations at 4°C with GST or GST-I2 bound to glutathione sepharose. Depletion was confirmed by PP1 immunoblotting; anti-actin was used to assure equal loading.

Recombinant protein affinity binding assay

Recombinant GST-C2 pro (20 μg) or GST-14-3-3 (ζ and ε, 20 μg) were bound to glutathione sepharose and incubated in egg extract. Sepharose-bound proteins were washed with buffer + 300 mM NaCl and 0.1% Triton-X, resolved by SDS-PAGE, and analyzed by immunoblotting.

14-3-3 release assay

20 μg GST-C2 pro bound to glutathione sepharose was incubated in extract + G6P to promote binding of endogenous 14-3-3ζ. Sepharose-bound proteins were retrieved and washed with low-salt buffer. GST-C2 pro with endogenous 14-3-3ζ was then added to fresh extract and samples of sepharose-bound proteins were retrieved over time, washed with buffer + 300 mM

NIH-PA Author Manuscript

NIH-PA Author Manuscript

NIH-PA Author Manuscript

NaCl and 0.1% Triton-X, eluted with SDS sample buffer, resolved by SDS-PAGE, and analyzed by immunoblotting with a pan-14-3-3 antibody.

Oocyte injection assays

pSP64T *Xenopus* full-length C2 cDNA templates were linearized with *Xba*I, and mRNA was generated using the Stratagene mRNA capping kit. Translation levels were tested with TNT reticulocyte lysate *in vitro* translation as described above or affinity precipitation from translationally-competent egg extract where specified.

Mouse C2 was cloned into pSP64T and mRNA was produced as previously described (Kurokawa et al., 2007). In brief, the cDNAs were linearized with *XbaI* and transcribed *in vitro* using the mMessage/mMachine capping kit (Ambion, Austin, TX). Mouse oocytes were collected and microinjected with mC2 mRNA as previously described (Fissore et al., 2002; Kurokawa et al., 2007).

Additional reagents

D-Glucose 6-phosphate sodium salt (Sigma-Aldrich) was used at 10 mM. Okadaic acid (Sigma-Aldrich) was used at 10 μM unless otherwise indicated. Glutathione Sepharose was purchased from Amersham Biosciences, Dynabeads Protein A from Invitrogen, Calmodulin and CaMKII from CalBiochem, and VDVAD-CHO from BioMol.

Supplementary Material

Refer to Web version on PubMed Central for supplementary material.

Acknowledgments

We thank Haian Fu for His-14-3-3ζ K49E plasmid, D. Ribar for technical assistance, and J. Bouten. This work was supported by NIH RO1 GM080333 to SK and HD51872 to RAF. LKN is a recipient of a Leukemia and Lymphoma Society Special Fellow Award. MRB is supported by MSTP Training Grant NIH GM07171 and a DOD BCRP Predoctoral Traineeship Award.

References

Baliga BC, Read SH, Kumar S. The biochemical mechanism of caspase-2 activation. Cell Death Differ 2004;11:1234–1241. [PubMed: 15297885]

Bergeron L, Perez GI, Macdonald G, Shi L, Sun Y, Jurisicova A, Varmuza S, Latham KE, Flaws JA, Salter JC, et al. Defects in regulation of apoptosis in caspase-2-deficient mice. Genes Dev 1998;12:1304–1314. [PubMed: 9573047]

Cohen PT. Protein phosphatase 1--targeted in many directions. J Cell Sci 2002;115:241–256. [PubMed: 11839776]

Danial NN, Gramm CF, Scorrano L, Zhang CY, Krauss S, Ranger AM, Datta SR, Greenberg ME, Licklider LJ, Lowell BB, et al. BAD and glucokinase reside in a mitochondrial complex that integrates glycolysis and apoptosis. Nature 2003;424:952–956. [PubMed: 12931191]

Danial NN, Korsmeyer SJ. Cell death: critical control points. Cell 2004;116:205–219. [PubMed: 14744432]

Datta SR, Katsov A, Hu L, Petros A, Fesik SW, Yaffe MB, Greenberg ME. 14-3-3 proteins and survival kinases cooperate to inactivate BAD by BH3 domain phosphorylation. Mol Cell 2000;6:41–51. [PubMed: 10949026]

de Schepper GG, van Noorden CJ, Houtkooper JM. Age-related changes of glucose-6-phosphate dehydrogenase activity in mouse oocytes. Histochem J 1987;19:467–470. [PubMed: 3440759]

Duan H, Dixit VM. RAIDD is a new ‘death’ adaptor molecule. Nature 1997;385:86–89. [PubMed: 8985253]

NIH-PA Author Manuscript

NIH-PA Author Manuscript

NIH-PA Author Manuscript

Egloff MP, Johnson DF, Moorhead G, Cohen PT, Cohen P, Barford D. Structural basis for the recognition of regulatory subunits by the catalytic subunit of protein phosphatase 1. Embo J 1997;16:1876–1887. [PubMed: 9155014]

Fissore RA, Kurokawa M, Knott J, Zhang M, Smyth J. Mechanisms underlying oocyte activation and postovulatory ageing. Reproduction 2002;124:745–754. [PubMed: 12530912]

Gasco M, Sullivan A, Repellin C, Brooks L, Farrell PJ, Tidy JA, Dunne B, Gusterson B, Evans DJ, Crook T. Coincident inactivation of 14-3-3sigma and p16INK4a is an early event in vulval squamous neoplasia. Oncogene 2002;21:1876–1881. [PubMed: 11896620]

Hanoux V, Pairault C, Bakalska M, Habert R, Livera G. Caspase-2 involvement during ionizing radiation-induced oocyte death in the mouse ovary. Cell Death Differ 2007;14:671–681. [PubMed: 17082817]

Kurokawa M, Yoon SY, Alfandari D, Fukami K, Sato K, Fissore RA. Proteolytic processing of phospholipase Czeta and [Ca2+]i oscillations during mammalian fertilization. Dev Biol 2007;312:407–418. [PubMed: 18028898]

Majewski N, Nogueira V, Bhaskar P, Coy PE, Skeen JE, Gottlob K, Chandel NS, Thompson CB, Robey RB, Hay N. Hexokinase-mitochondria interaction mediated by Akt is required to inhibit apoptosis in the presence or absence of Bax and Bak. Mol Cell 2004;16:819–830. [PubMed: 15574336]

Margolis SS, Perry JA, Weitzel DH, Freel CD, Yoshida M, Haystead TA, Kornbluth S. A role for PP1 in the Cdc2/Cyclin B-mediated positive feedback activation of Cdc25. Mol Biol Cell 2006;17:1779–1789. [PubMed: 16467385]

Margolis SS, Walsh S, Weiser DC, Yoshida M, Shenolikar S, Kornbluth S. PP1 control of M phase entry exerted through 14-3-3-regulated Cdc25 dephosphorylation. Embo J 2003;22:5734–5745. [PubMed: 14592972]

Nomura M, Shimizu S, Sugiyama T, Narita M, Ito T, Matsuda H, Tsujimoto Y. 14-3-3 Interacts directly with and negatively regulates pro-apoptotic Bax. J Biol Chem 2003;278:2058–2065. [PubMed: 12426317]

Nutt LK, Margolis SS, Jensen M, Herman CE, Dunphy WG, Rathmell JC, Kornbluth S. Metabolic regulation of oocyte cell death through the CaMKII-mediated phosphorylation of caspase-2. Cell 2005;123:89–103. [PubMed: 16213215]

Panaretakis T, Laane E, Pokrovskaja K, Bjorklund AC, Moustakas A, Zhivotovsky B, Heyman M, Shoshan MC, Grander D. Doxorubicin requires the sequential activation of caspase-2, protein kinase Cdelta, and c-Jun NH2-terminal kinase to induce apoptosis. Mol Biol Cell 2005;16:3821–3831. [PubMed: 15917298]

Pastorino JG, Shulga N, Hoek JB. Mitochondrial binding of hexokinase II inhibits Bax-induced cytochrome c release and apoptosis. J Biol Chem 2002;277:7610–7618. [PubMed: 11751859]

Rathmell JC, Fox CJ, Plas DR, Hammerman PS, Cinalli RM, Thompson CB. Akt-directed glucose metabolism can prevent Bax conformation change and promote growth factor-independent survival. Mol Cell Biol 2003;23:7315–7328. [PubMed: 14517300]

Read SH, Baliga BC, Ekert PG, Vaux DL, Kumar S. A novel Apaf-1-independent putative caspase-2 activation complex. J Cell Biol 2002;159:739–745. [PubMed: 12460989]

Rittinger K, Budman J, Xu J, Volinia S, Cantley LC, Smerdon SJ, Gamblin SJ, Yaffe MB. Structural analysis of 14-3-3 phosphopeptide complexes identifies a dual role for the nuclear export signal of 14-3-3 in ligand binding. Mol Cell 1999;4:153–166. [PubMed: 10488331]

Robertson JD, Enoksson M, Suomela M, Zhivotovsky B, Orrenius S. Caspase-2 acts upstream of mitochondria to promote cytochrome c release during etoposide-induced apoptosis. J Biol Chem 2002;277:29803–29809. [PubMed: 12065594]

Shenolikar S. Protein serine/threonine phosphatases--new avenues for cell regulation. Annu Rev Cell Biol 1994;10:55–86. [PubMed: 7888183]

Smythe C, Newport JW. Systems for the study of nuclear assembly, DNA replication, and nuclear breakdown in Xenopus laevis egg extracts. Methods Cell Biol 1991;35:449–468. [PubMed: 1664032]

Sunayama J, Tsuruta F, Masuyama N, Gotoh Y. JNK antagonizes Akt-mediated survival signals by phosphorylating 14-3-3. J Cell Biol 2005;170:295–304. [PubMed: 16009721]

Tinel A, Tschopp J. The PIDDosome, a protein complex implicated in activation of caspase-2 in response to genotoxic stress. Science 2004;304:843–846. [PubMed: 15073321]

NIH-PA Author Manuscript

NIH-PA Author Manuscript

NIH-PA Author Manuscript

Tsuruta F, Sunayama J, Mori Y, Hattori S, Shimizu S, Tsujimoto Y, Yoshioka K, Masuyama N, Gotoh Y. JNK promotes Bax translocation to mitochondria through phosphorylation of 14-3-3 proteins. Embo J 2004;23:1889–1899. [PubMed: 15071501]

Vietri M, Bianchi M, Ludlow JW, Mittnacht S, Villa-Moruzzi E. Direct interaction between the catalytic subunit of Protein Phosphatase 1 and pRb. Cancer Cell Int 2006;6:3. [PubMed: 16466572]

Wakula P, Beullens M, Ceulemans H, Stalmans W, Bollen M. Degeneracy and function of the ubiquitous RVXF motif that mediates binding to protein phosphatase-1. J Biol Chem 2003;278:18817–18823. [PubMed: 12657641]

Yaffe MB, Rittinger K, Volinia S, Caron PR, Aitken A, Leffers H, Gamblin SJ, Smerdon SJ, Cantley LC. The structural basis for 14-3-3:phosphopeptide binding specificity. Cell 1997;91:961–971. [PubMed: 9428519]

Yang X, Lee WH, Sobott F, Papagrigoriou E, Robinson CV, Grossmann JG, Sundstrom M, Doyle DA, Elkins JM. Structural basis for protein-protein interactions in the 14-3-3 protein family. Proc Natl Acad Sci U S A 2006;103:17237–17242. [PubMed: 17085597]

Zha J, Harada H, Yang E, Jockel J, Korsmeyer SJ. Serine phosphorylation of death agonist BAD in response to survival factor results in binding to 14-3-3 not BCL-X(L). Cell 1996;87:619–628. [PubMed: 8929531]

Zhang L, Wang H, Liu D, Liddington R, Fu H. Raf-1 kinase and exoenzyme S interact with 14-3-3zeta through a common site involving lysine 49. J Biol Chem 1997;272:13717–13724. [PubMed: 9153224]

Zhao Y, Altman BJ, Coloff JL, Herman CE, Jacobs SR, Wieman HL, Wofford JA, Dimascio LN, Ilkayeva O, Kelekar A, et al. Glycogen synthase kinase 3alpha and 3beta mediate a glucose-sensitive antiapoptotic signaling pathway to stabilize Mcl-1. Mol Cell Biol 2007;27:4328–4339. [PubMed: 17371841]

NIH-PA Author Manuscript
NIH-PA Author Manuscript
NIH-PA Author Manuscript

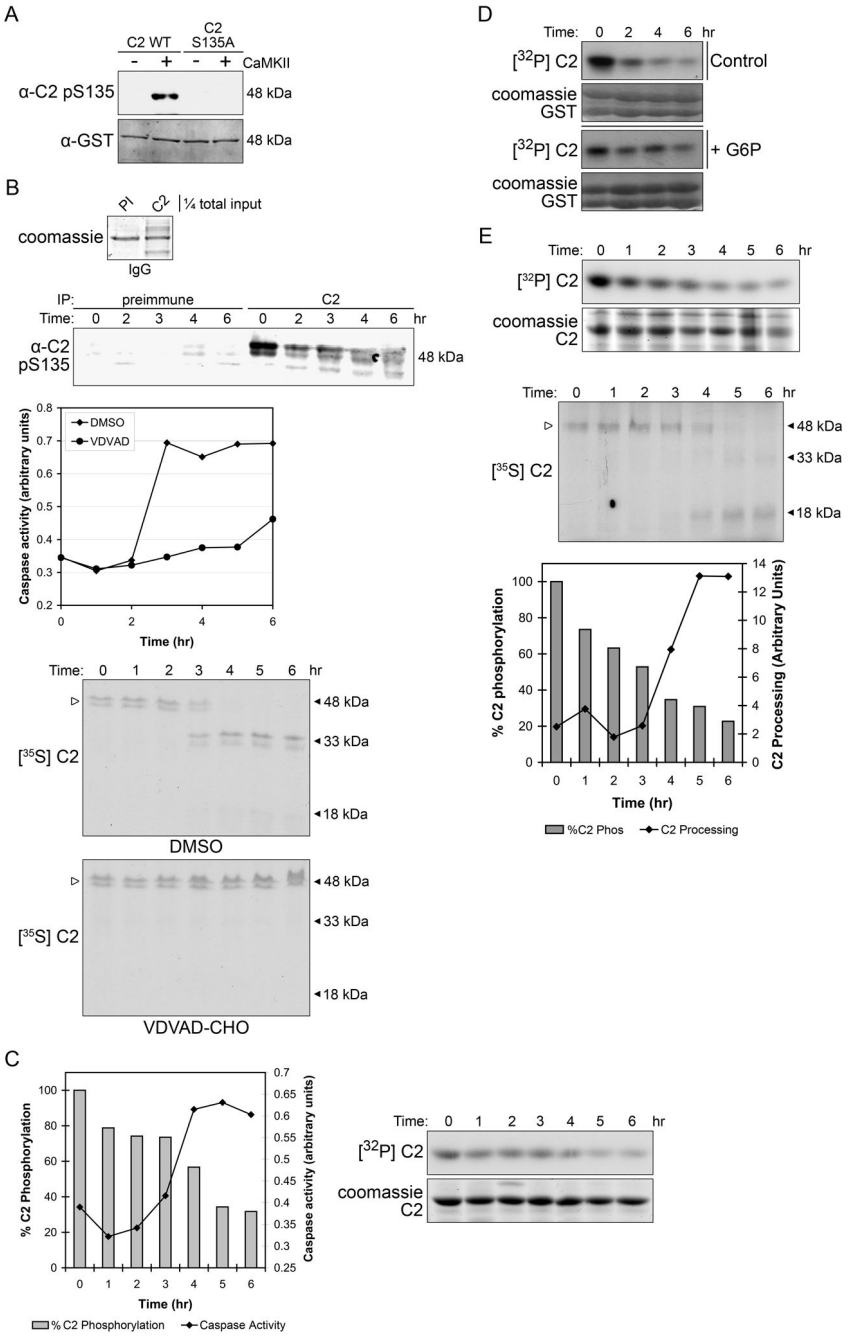

Figure 1. Caspase-2 S135 dephosphorylation is sensitive to metabolism

(A) Glutathione sepharose-bound GST-C2 pro WT or S135A was phosphorylated *in vitro* ± recombinant CaMKII. Samples were resolved by SDS-PAGE and immunoblotted using an antibody specific to *Xenopus* C2 pS135.

(B) Anti-C2 and its corresponding preimmune serum were titrated to determine equal IgG loading (upper panel). Extracts treated with 100 μM VDVAD-CHO were immunoprecipitated at the indicated time points for one hour using preimmune- or C2-IgG bound to Dynabeads Protein A. Samples were resolved by SDS-PAGE and immunoblotted for C2 pS135 (second panel). In parallel, extracts were analyzed for processing of radiolabeled *in vitro*-translated

NIH-PA Author Manuscript

NIH-PA Author Manuscript

NIH-PA Author Manuscript

full-length C2 or C3 activity (lower panels). White arrow = full-length C2; PI = preimmune; IP = immunoprecipitate. n = 3

(C) Left panel: Extracts were analyzed for C3 activity over time using the caspase substrate Ac-DEVD-pNA. Right panel: In parallel, GST-C2 pro was prephosphorylated with CaMKII and [γ-^{32}P]ATP; sepharose-bound proteins were incubated in extract over time and samples were resolved by SDS-PAGE and detected by autoradiography. Data are demonstrated quantitatively in the left panel. n=5

(D) Glutathione sepharose-bound GST-C2 pro was prephosphorylated with [γ-^{32}P]ATP as described in (A) and sepharose-bound proteins were incubated in extract ± G6P. Samples were taken over time and detected by autoradiography. In parallel, extracts ± G6P were analyzed for C3 activity using Ac-DEVD-pNA (Supplemental Data). n = 3

(E) Top panel: GST-C2 pro pS135 was analyzed over time as described in (A). Middle panel: In parallel, processing of full-length C2 was examined by autoradiography. Quantitation is provided (bottom panel). White arrow = full-length C2. n = 3

NIH-PA Author Manuscript
NIH-PA Author Manuscript
NIH-PA Author Manuscript

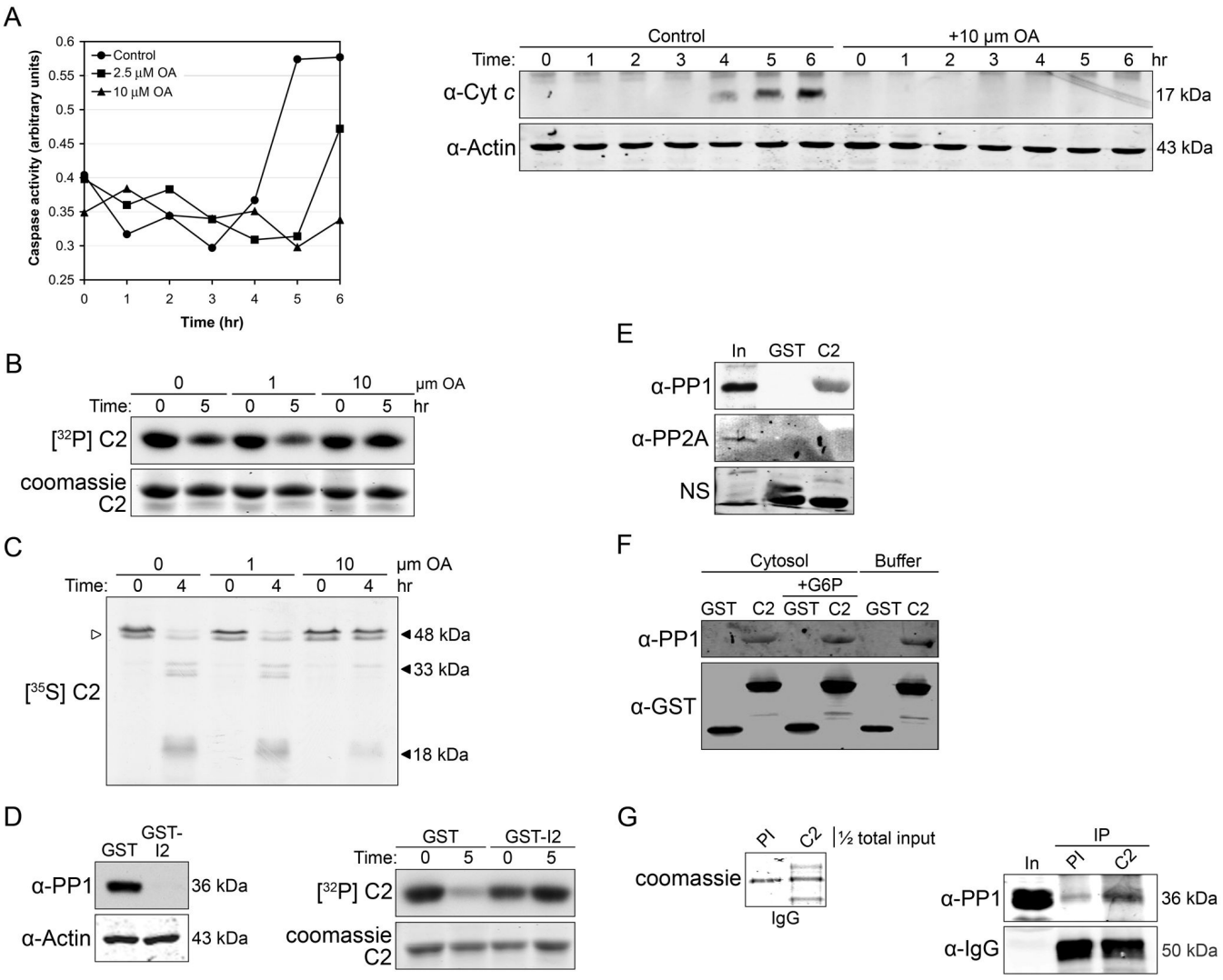

Figure 2. Caspase-2 dephosphorylation is mediated by PP1

(A) Left panel: Control- or OA-treated extracts were analyzed for C3 activity with the substrate Ac-DEVD-pNA. Right panel: Cyt *c* release was measured in control- or OA-treated samples. Cytosol was analyzed by SDS-PAGE and immunoblotted with an anti-cyt *c* antibody and anti-actin. OA = okadaic acid. n = 3

(B) GST-C2 pro bound to glutathione sepharose was prephosphorylated with [γ-^{32}P]ATP. Sepharose-bound proteins were incubated in extracts ± OA, and samples were resolved by SDS-PAGE and detected by autoradiography. n = 3

(C) Extracts were treated with OA and processing of radiolabeled full-length C2 was examined by autoradiography. White arrow = full-length C2. n = 3

(D) Glutathione sepharose-bound GST-C2 pro was prephosphorylated with [γ-^{32}P]ATP. In parallel, extracts were depleted of endogenous PP1 with GST- or GST-Inhibitor-2 (I2) (left panel). Prephosphorylated GST-C2 pro was incubated in depleted extracts and samples were retrieved over time and detected by autoradiography (right panel). n = 4

(E) Glutathione sepharose-bound GST or GST-C2 pro was incubated in extract and affinity-purified proteins were resolved by SDS-PAGE and immunoblotted for PP1. The membrane was co-probed for PP2A. In = input; NS = non-specific.

NIH-PA Author Manuscript

NIH-PA Author Manuscript

NIH-PA Author Manuscript

(F) (First four lanes): Glutathione sepharose-bound GST or GST-C2 pro was incubated in extract ± G6P and affinity-purified proteins were resolved by SDS-PAGE and immunoblotted for PP1. (Right two lanes): Glutathione sepharose-bound GST or GST-C2 pro was incubated in buffer with recombinant PP1 catalytic domain. Sepharose-bound proteins were resolved by SDS-PAGE and immunoblotted for PP1.

(G) Anti-C2 and its corresponding preimmune serum were titrated to determine equal IgG loading (left panel). Extracts were immunoprecipitated using preimmune- or C2-IgG bound to Dynabeads Protein A. Immunoprecipitates were resolved by SDS-PAGE and immunoblotted for PP1; rabbit IgG heavy chain is also shown. In = input; PI = preimmune; IP = immunoprecipitate.

NIH-PA Author Manuscript

NIH-PA Author Manuscript

NIH-PA Author Manuscript

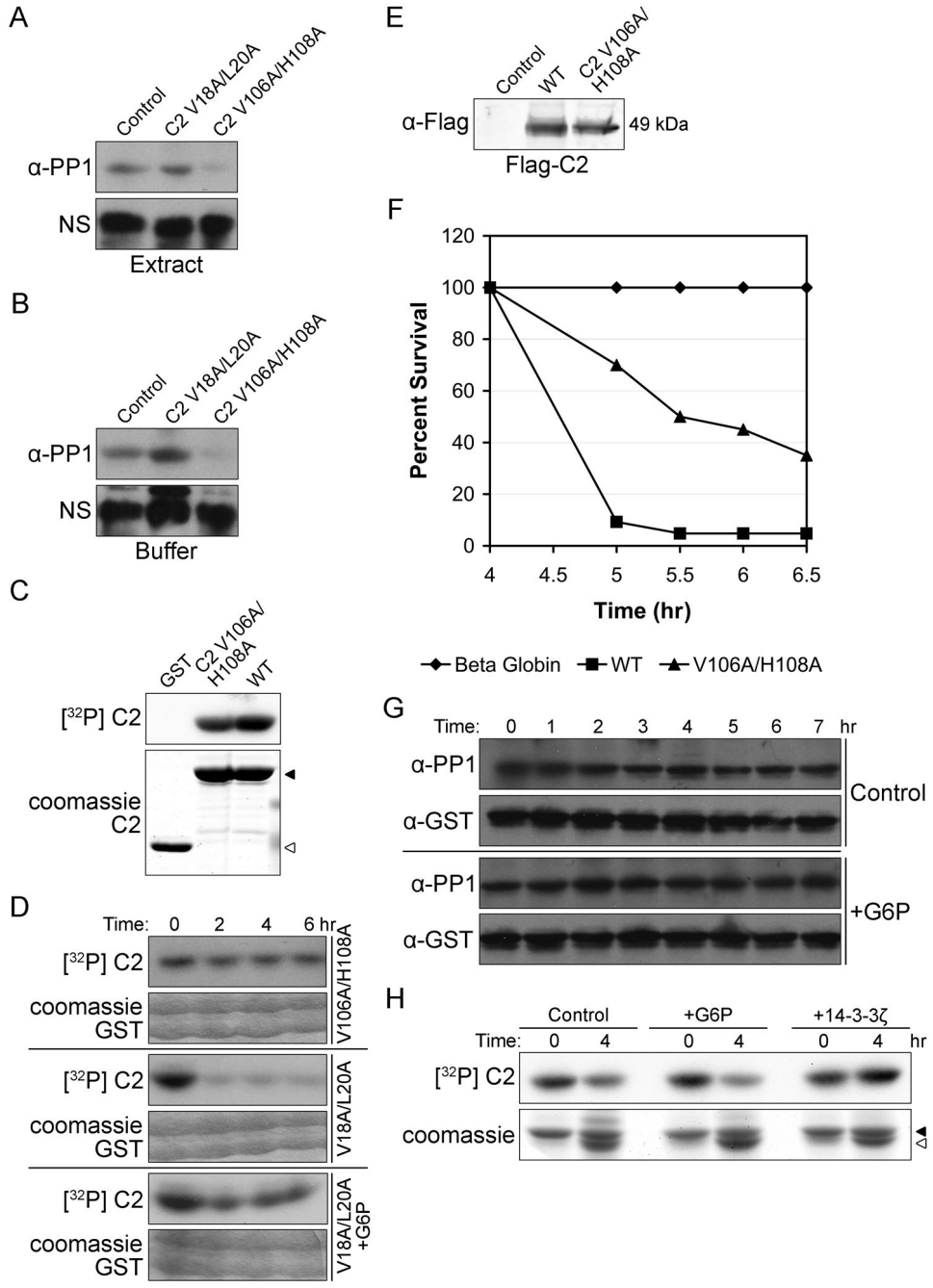

Figure 3. PP1 binding is required for caspase-2 activation

(A) Glutathione sepharose-bound GST-C2 pro WT, V18A/L20A, or V106A/H108A was incubated in extract, resolved by SDS-PAGE, and immunoblotted for PP1. NS = non-specific.

(B) Glutathione sepharose-bound GST-C2 pro WT, V18A/L20A, or V106A/H108A was incubated in buffer with recombinant PP1 catalytic domain. Sepharose-bound proteins were resolved by SDS-PAGE and immunoblotted for PP1. NS = non-specific.

(C) Glutathione sepharose-bound GST, GST-C2 pro WT, or V106A/H108A was prephosphorylated with [γ-^{32}P]ATP. Samples were resolved by SDS-PAGE and examined by autoradiography. Black arrow = GST-C2 pro; white arrow = GST.

NIH-PA Author Manuscript

NIH-PA Author Manuscript

NIH-PA Author Manuscript

(D) Glutathione sepharose-bound GST-C2 pro V106A/H108A or V18A/L20A was prephosphorylated with [γ-^{32}P]ATP and incubated in extract ± G6P. Samples were resolved by SDS-PAGE and detected by autoradiography. n = 3
(E) Flag-tagged full-length C2 WT or V106A/H108A mRNA was incubated in translationally-competent extract + 100 μM VDVAD-CHO. Translated flag-tagged C2 was retrieved with anti-flag agarose and samples were analyzed by immunoblotting with anti-flag.
(F) Percent survival of *Xenopus* oocytes microinjected with β-globin, full-length C2 WT, or V106A/H108A mRNA. Equivalent levels of C2 mRNA expression were determined as described in (E). n = 3
(G) Glutathione sepharose-bound GST-C2 pro was incubated in extract ± G6P and samples were retrieved over time and immunoblotted for PP1 and GST. n = 3
(H) Glutathione sepharose-bound GST-C2 pro was prephosphorylated with [γ-^{32}P]ATP and incubated in buffer with His-PP1 pre-incubated in extract ± G6P or excess His-14-3-3ζ (27 μM). Samples were analyzed by SDS-PAGE and autoradiography. Black arrow = GST-C2 pro; white arrow = His-PP1. n = 4

NIH-PA Author Manuscript
NIH-PA Author Manuscript
NIH-PA Author Manuscript

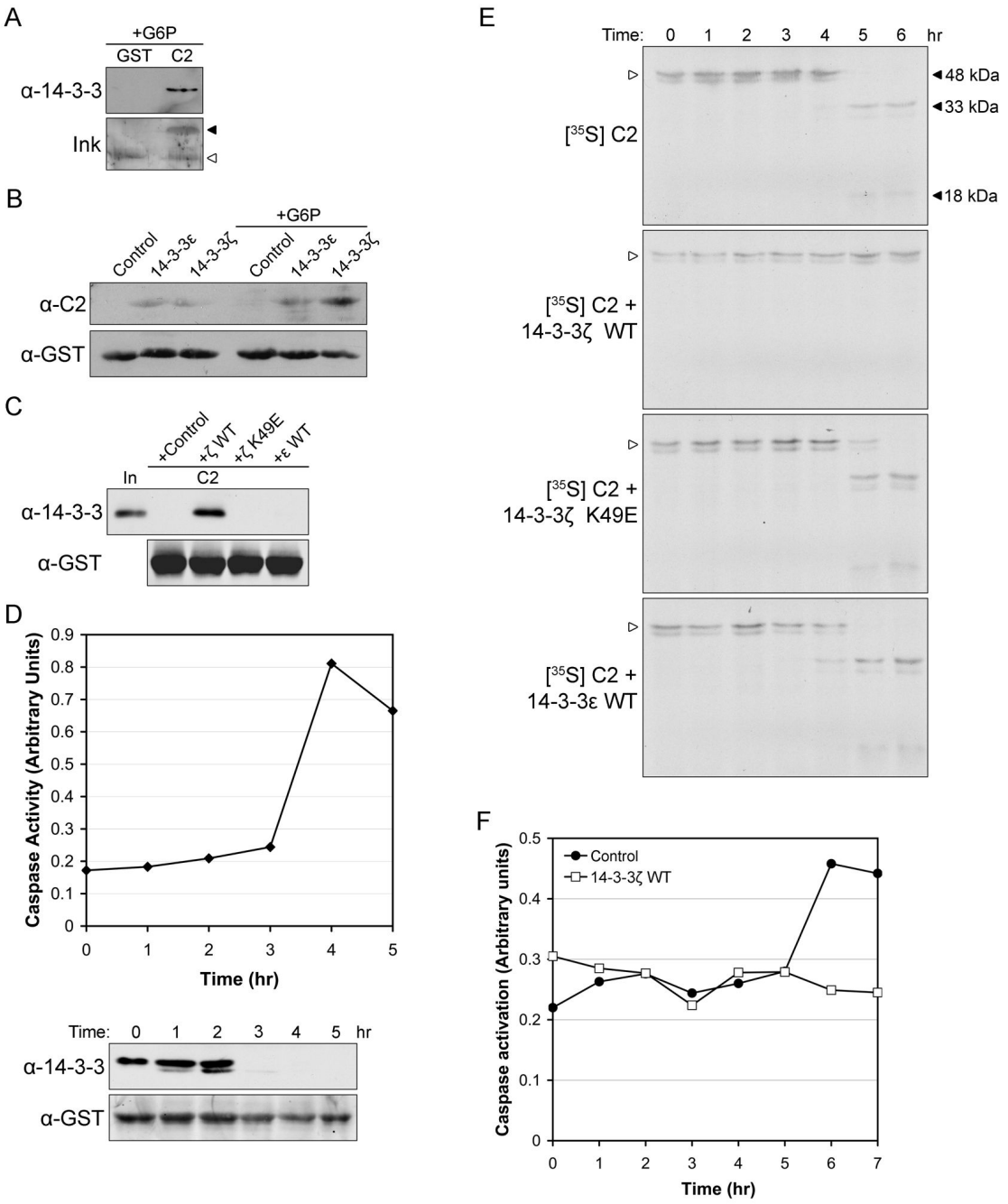

Figure 4. Caspase-2 binds 14-3-3ζ

(A) Glutathione sepharose-bound GST or GST-C2 pro was incubated in extract + G6P. Affinity-purified proteins were resolved by SDS-PAGE and immunoblotted with a pan-14-3-3 antibody. Black arrow = GST-C2 pro; white arrow = GST.

(B) Glutathione sepharose-bound GST, GST-14-3-3ε, or GST-14-3-3ζ was incubated in extract ± G6P, and sepharose-bound proteins were resolved by SDS-PAGE and immunoblotted for *Xenopus* C2.

(C) Glutathione sepharose-bound GST-C2 pro was phosphorylated at S135 and incubated with either control conditions, His-14-3-3ζ WT, His-14-3-3ζ K49E, or His-14-3-3ε in buffer.

NIH-PA Author Manuscript

NIH-PA Author Manuscript

NIH-PA Author Manuscript

Sepharose-bound proteins were analyzed by SDS-PAGE and immunblotted with a pan-14-3-3 antibody. In = input.

(D) Upper panel: Extracts were analyzed for C3 activity using the caspase substrate Ac-DEVD-pNA. Lower panel: In parallel, glutathione sepharose-bound GST-C2 pro was incubated in extract + G6P to promote binding of endogenous 14-3-3ζ, and this construct was then incubated in fresh extract. Samples were retrieved and analyzed for 14-3-3 binding. n = 4

(E) Extract was incubated with radiolabeled full-length *in vitro*-translated C2 in the presence of either control conditions, His-14-3-3ζ WT, His-14-3-3ζ K49E, or His-14-3-3ε. Samples were analyzed for C2 processing by autoradiography. White arrow = full-length C2. n = 3

(F) Extracts ± His-14-3-3ζ WT were analyzed for C3 activity using the caspase substrate Ac-DEVD-pNA. n = 3

NIH-PA Author Manuscript

NIH-PA Author Manuscript

NIH-PA Author Manuscript

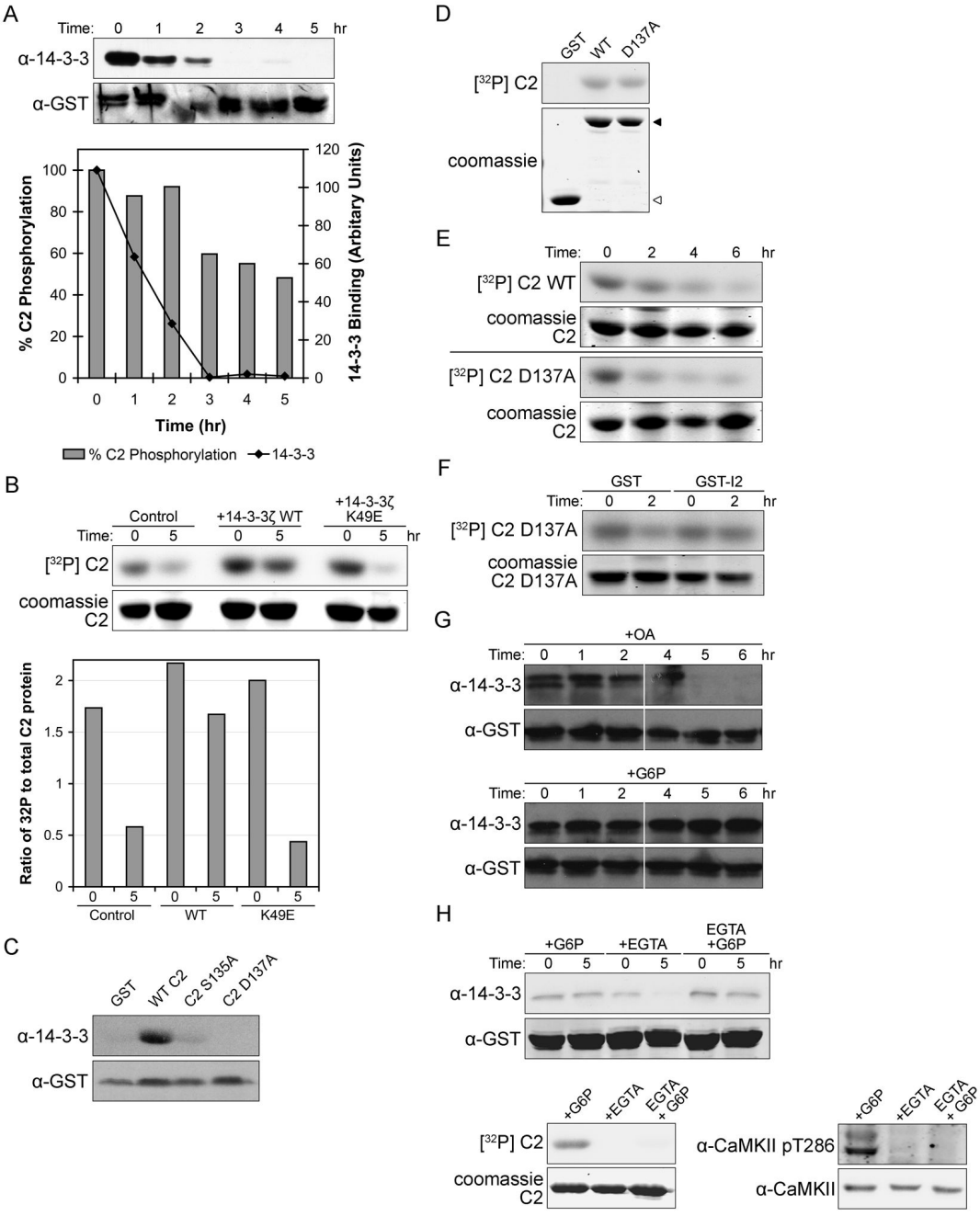

Figure 5. 14-3-3ζ binding prevents caspase-2 dephosphorylation

(A) Upper panel: Glutathione sepharose-bound GST-C2 pro was pre-bound to endogenous 14-3-3ζ and then incubated in fresh extract; samples were analyzed for 14-3-3 binding. The membrane was co-probed with a GST antibody. In parallel, glutathione sepharose-bound GST-C2 pro was prephosphorylated with [γ-^{32}P]ATP and incubated in extract. Samples were analyzed by autoradiography (data not shown). The results of these experiments are depicted quantitatively (lower panel). n = 3

(B) Upper panel: Glutathione sepharose-bound GST-C2 pro was prephosphorylated with [γ-^{32}P]ATP and incubated in extracts with control conditions, His-14-3-3ζ WT, or

NIH-PA Author Manuscript

NIH-PA Author Manuscript

NIH-PA Author Manuscript

His-14-3-3ζ. Samples were analyzed by autoradiography. Quantitation of GST-C2 pro phosphorylation is provided relative to total protein (lower panel). n = 4

(C) Glutathione sepharose-bound GST, GST-C2 pro WT, S135A, or D137A was incubated in extract + G6P and affinity-purified proteins were resolved by SDS-PAGE and immunoblotted for 14-3-3.

(D) Glutathione sepharose-bound GST, GST-C2 pro WT, or D137A was phosphorylated with CaMKII and [γ-^{32}P]ATP in buffer. Sepharose-bound proteins were analyzed by autoradiography. Black arrow = GST-C2 pro; white arrow = GST.

(E) Glutathione sepharose-bound GST-C2 pro WT or D137A was prephosphorylated with [γ-^{32}P]ATP and incubated in extracts. Samples were retrieved over time and analyzed by autoradiography. n = 3

(F) Glutathione sepharose-bound GST-C2 pro D137A was prephosphorylated with [γ-^{32}P] ATP. In parallel, extracts were depleted of endogenous PP1 with GST- or GST-I2 (experiment 2D was performed in parallel; extent of PP1 depletion is demonstrated in Fig. 2D). Prephosphorylated GST-C2 pro D137A was incubated in depleted extracts and samples were resolved by SDS-PAGE and detected by autoradiography. n = 2

(G) Glutathione sepharose-bound GST-C2 pro was incubated in extract + G6P to promote binding of endogenous 14-3-3ζ. Sepharose-bound GST-C2 pre-bound to endogenous 14-3-3ζ as incubated in fresh extract in the presence of either OA or G6P. Sepharose-bound proteins were analyzed for 14-3-3 binding by immunoblotting. n = 3

(H) Upper panel: Glutathione sepharose-bound GST-C2 pro was pre-bound to endogenous 14-3-3ζ and incubated in extract ± G6P and EGTA (5 mM). Samples were analyzed for 14-3-3 binding by immunoblotting. Lower left panel: In parallel, GST-C2 pro was incubated in extracts with [γ-^{32}P]ATP ± G6P and EGTA; samples were analyzed by autoradiography. Lower right panel: Samples of G6P and EGTA-treated extracts were analyzed for CaMKII activation by immunoblotting for CaMKII pT286. n = 3

NIH-PA Author Manuscript

NIH-PA Author Manuscript

NIH-PA Author Manuscript

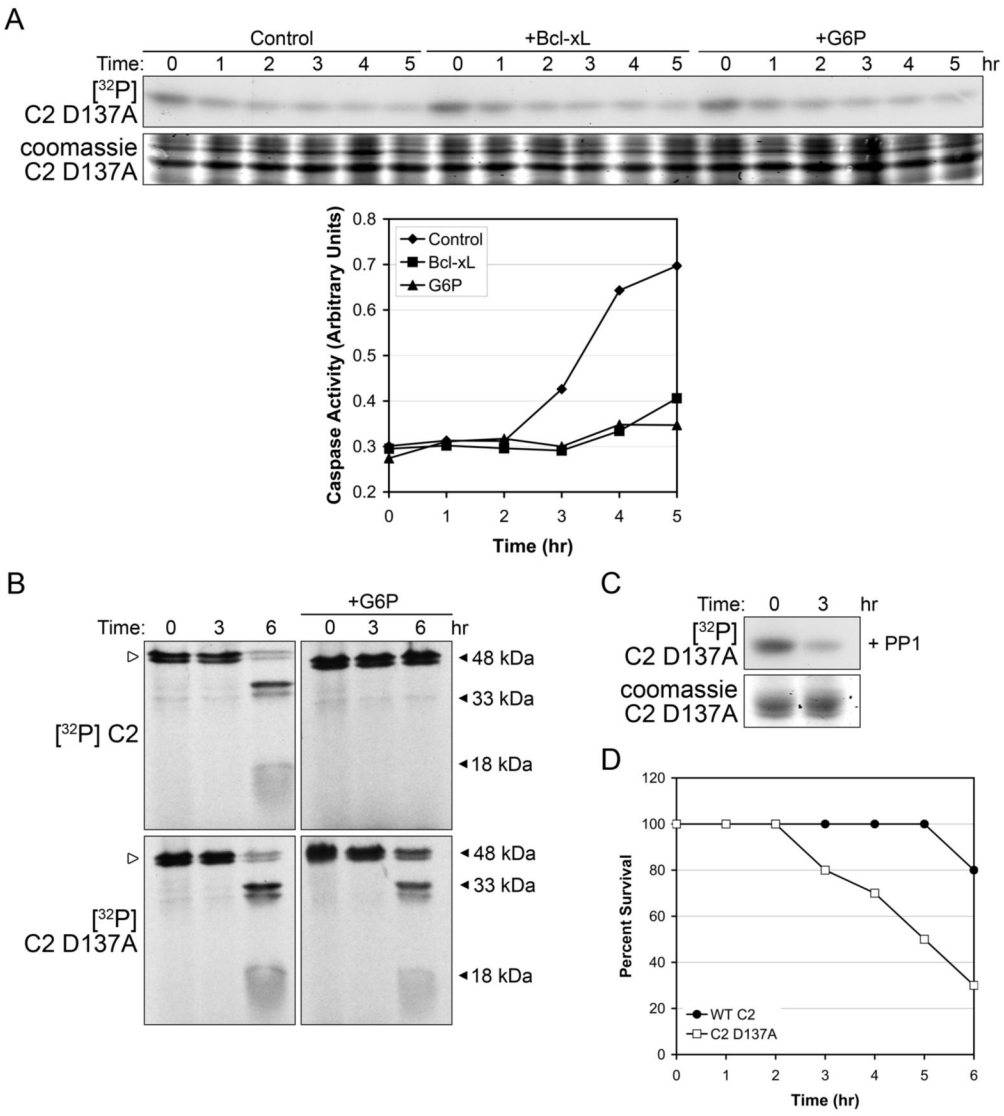

Figure 6. The interaction between caspase-2 and 14-3-3ζ is metabolically regulated

(A) Upper panel: Glutathione sepharose-bound GST-C2 pro D137A was prephosphorylated with [γ-^{32}P]ATP and incubated in extracts ± G6P or Bcl-xL. Samples of sepharose-bound proteins were analyzed by autoradiography. Lower panel: In parallel, extracts treated with the same conditions were analyzed for C3 activity using the caspase substrate Ac-DEVD-pNA. n = 3

(B) Radiolabeled *in vitro* translated full-length C2 WT or D137 was incubated in extracts ± G6P. Samples were retrieved over time and analyzed by SDS-PAGE and autoradiography.

(C) Glutathione sepharose-bound GST-C2 pro D137A was prephosphorylated with [γ-^{32}P] ATP and incubated in buffer with His-PP1 that had been pre-incubated in extract. Samples of sepharose-bound proteins were analyzed by autoradiography. n = 2

(D) Percent survival of *Xenopus* oocytes microinjected with full-length C2 WT or D137A mRNA. n = 3

NIH-PA Author Manuscript

NIH-PA Author Manuscript

NIH-PA Author Manuscript

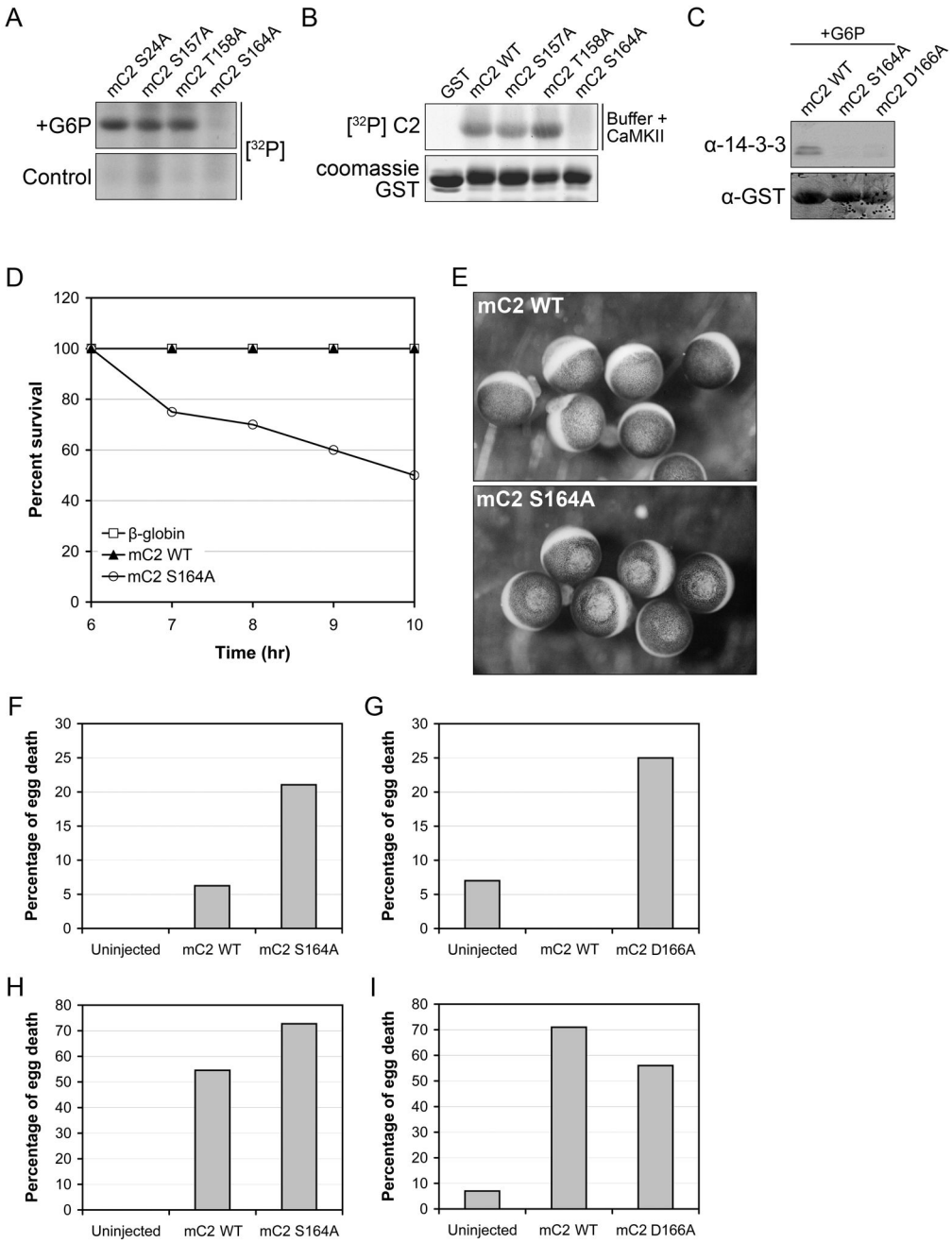

Figure 7. Conservation of caspase-2 metabolic regulation in the mouse egg

(A) Glutathione sepharose-bound GST-mC2 pro WT, S24A, S157A, T158A, or S164A was incubated in *Xenopus* extracts ± G6P and [γ-^{32}P]ATP. Sepharose-bound proteins were analyzed by autoradiography.

(B) Glutathione sepharose-bound GST-mC2 pro WT, S157A, T158A, or S164A was phosphorylated *in vitro* with CaMKII and [γ-^{32}P]ATP. Sepharose-bound proteins were analyzed by autoradiography.

(C) Glutathione sepharose-bound GST-mC2 pro WT, S164A, or D166A was incubated in *Xenopus* extract + G6P. Sepharose-bound proteins were analyzed by SDS-PAGE and immunoblotted for 14-3-3.

NIH-PA Author Manuscript

NIH-PA Author Manuscript

NIH-PA Author Manuscript

(D) Percent survival of *Xenopus* oocytes microinjected with mC2 WT, S164A, or β-globin mRNA. n = 3
(E) *Xenopus* oocytes microinjected with mC2 WT or S164A mRNA as described in (D) shown as representative micrographs. n = 3
(F) Percent death of fresh mouse eggs microinjected with mC2 WT or S164A mRNA, 19 hrs post-injection. n = 3
(G) Percent death of fresh mouse eggs microinjected with mC2 WT or D166A mRNA (24 hrs post-injection; this is a separate experiment from (E) and the time course of death varied somewhat between batches of eggs). n = 3
(H) Percent death of aged mouse eggs microinjected with mC2 WT or S164A mRNA, 8 hrs post-injection. n = 3
(I) Percent death of aged mouse eggs microinjected with mC2 WT or D166A mRNA, 6 hrs post-injection (note that death of the aged eggs in G and H was consistently accelerated relative to the fresh postovulatory eggs). n = 3